Calculations of hydrogen coverage on single-walled carbon nanotubes: Dependence on nanotube size, temperature, and pressure

Xiaobao Yang and Jun Ni
Department of Physics and Key Laboratory of Atomic and Molecular Nanoscience (Ministry of Education), Tsinghua University, Beijing 100084, People's Republic of China

(Received 18 July 2006; revised manuscript received 13 September 2006; published 30 November 2006)

We have investigated the stability of various hydrogenated single-walled carbon nanotubes. We find that the storage capacity of hydrogen depends significantly on the diameters of carbon nanotubes. Full hydrogen coverage can be reached for nanotubes with small size, while for nanotubes with large size, the saturation coverage is lower than 1. We have calculated the variation of the hydrogen coverage with the change of temperature and pressure. In particular, we find that nanotubes with diameters of about 1 nm can achieve a coverage of 80% at ambient temperature and low pressure, which is in agreement with the experimental results.

DOI: 10.1103/PhysRevB.74.195437 PACS number(s): 61.46.−w, 68.43.De, 68.43.−h

I. INTRODUCTION

The safe and compact storage of hydrogen is of great interest in theoretical and experimental research. Carbon nanotubes, one of the most promising materials, are reported to be highly efficient for gas and alkali-atom storage.[1–8] The curved surface of carbon nanotubes and the empty space inside nanotubes increase the storage capacity greatly. Hydrogen storage capacity is predicted to exceed 14 wt % in (10,10) nanotubes.[4] Chen *et al.* reported that intercalated alkali atoms in carbon nanotubes would significantly enhance the hydrogen storage.[5] A theoretical study shows that alkali atoms enlarge the distance between carbon nanotubes and attract hydrogen molecules, which leads to higher hydrogen storage.[6] Zhao *et al.* reported that transition-metal-dispersed C_{60} and $C_{48}B_{12}$ are considered to be a novel hydrogen storage medium with H_2 density of 9 wt %.[7] Yildirim *et al.* predicted that each Ti atom coated on carbon nanotubes can bind up to four hydrogen molecules and the decorated nanotubes can adsorb up to 8 wt % hydrogen at high Ti coverage.[8]

Recent studies show that hydrogen molecule physisorption is rather weak with an energy barrier of 2.7 eV for H_2 dissociation on pristine tubes.[9] The sidewalls of carbon nanotubes make H_2 molecules difficult to enter inside and the H_2 molecule storage requires high pressure and very low temperature,[10,11] which is impractical for applications. Atomic hydrogen has been used as a source to overcome the difficulty. Density functional theory (DFT) calculations show that fully exohydrogenated carbon nanotubes are stable up to the radius of the (8,8) tube, with the binding energy inversely proportional to the diameter.[12] For the (5,5) tube, it has been reported that exohydrogenated nanotubes are stable with hydrogen coverage $x \geqslant 0.3$.[13,14] For (9,0), (10,0), and (5,5) tubes, the hydrogen adsorption both inside and outside the tubes is more stable than the one with hydrogen only outside.[15] Experimental results show that the hydrogenation outside the single-walled carbon nanotubes (SWCNT's) is more practical and the hydrogen coverage varies with the environment conditions. Nikitin *et al.* managed a 65 ± 15 at. % hydrogenation of carbon atoms in SWCNT's with diameters from 1 to 1.8 nm.[16] C-H bonds are formed at room temperature and broken at 600 °C, showing that the hydrogenation is a reversible process.

The process of hydrogen adsorption on the carbon nanotubes is changed under various circumstances: (i) The interaction between hydrogen atoms and carbon nanotubes depends on the diameters of the tubes. It is not clear how the coverage of hydrogen atoms depends on the size and chirality of the tubes. (ii) To understand the process of hydrogen adsorption on carbon nanotubes, it is important to know how the hydrogen coverage depends on temperature and pressure. In this work, we have studied the adsorption of hydrogen atoms on the walls of carbon nanotubes. We find that the storage capacity of hydrogen depends strongly on the diameters of carbon nanotubes. Based on the envelope profile of the intercalation energies, we have obtained a variation of the hydrogen coverage as functions of temperature and pressure. We show that the hydrogen storage is more efficient for the carbon nanotubes with smaller size.

II. METHODS

We have performed calculations of the total energies of the exohydrogenated carbon nanotubes with various coverages using VASP (Vienna *ab initio* simulation package).[17] The approach is based on an iterative solution of the Kohn-Sham equations of the density functional theory in a plane-wave basis set with Vanderbilt ultrasoft pseudopotentials.[18] We use the exchange correlation with generalized gradient approximation given by Perdew *et al.*[19] We set the plane-wave cutoff energy to be 420 eV and the convergence of the force on each atom to be less than 0.01 eV/Å. The Monkhorst-Pack scheme is used to sample the Brillouin zone.[20] Optimization of the lattice constants and the atom coordinates is made by minimization of the total energy. All structures are fully relaxed with a mesh of $1 \times 1 \times 9$, and the mesh of **k** space is increased to $1 \times 1 \times 20$ to obtain accurate energies with atoms fixed after relaxations.

The diameters of carbon nanotubes in the recent hydrogen storage experiments range from 1 to 1.8 nm.[16] We consider carbon nanotubes with different chiralities, such as (6,0), (8,0), (6,6), (12,0), (8,8), and (16,0), whose diameters range from 0.5 to 1.3 nm. The unit cells for the hydrogenated

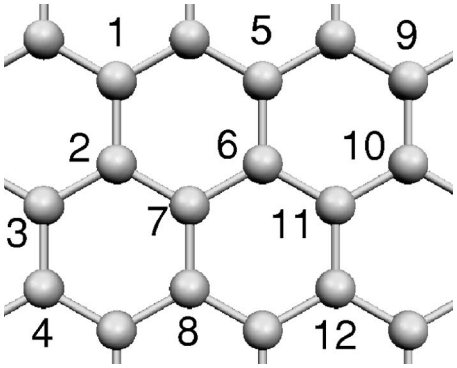

FIG. 1. The sites for the adsorption of hydrogen atoms on the walls of carbon nanotubes.

carbon nanotubes are taken as two period lengths of the tubes in our calculations. Our calculations show that hydrogen atoms prefer to be adsorbed at the top sites outside the walls of tubes, which is in agreement with the results of other works.[12,13] We define the binding energy E_b as follows: $E_b=(E_{SWCNT}+n_HE_H-E_{H\text{-}SWCNT})/n_H$, where E_{SWCNT} is the total energy of a pristine carbon nanotube, E_H is the total energy of an isolated H atom, and $E_{H\text{-}SWCNT}$ is the energy of the hydrogenated nanotube. n_H is the number of hydrogen atoms. For a fixed coverage, the structure with higher E_b is more stable.

III. RESULTS

In general, there are a lot of possible atomic configurations for hydrogen adsorbates on SWCNT's. In order to obtain stable configurations, we first consider isolated patterns of hydrogen atoms outside the carbon nanotubes and take the (8,0) tube as an example. For an isolated hydrogen atom on the wall of the (8,0) tube, E_b is 1.51 eV. The length of the CH bond is 1.11 Å and the three CCH bond angles are 106.7°, 107.9°, and 107.9°, which are close to the ideal tetrahedral sp^3 bond angle of 109.5°. When two hydrogen atoms are added to the wall of the tube, there are three possible configurations: the 1-2, 2-3, and 3-7 neighboring configurations, as is shown in Fig. 1. The lengths of the CH bonds are 1.11 Å for these three cases. The average CCH bond angles are 107.5°, 105.5°, and 106.6°. E_b of the three cases are 2.37, 2.08, and 1.55 eV, respectively. It is shown that two hydrogen atoms prefer to form a dimer on two neighboring carbon atoms. For the nanotube with an isolated hydrogen atom adsorbed, the C-C π bond is broken by the hydrogen atom and the nearest site is made very active, which leads to a stable hydrogen dimer. The H-H distances for these three cases are 2.22, 2.16, and 3.68 Å, which are much larger than the bond length of a hydrogen molecule (0.75 Å). Thus the interactions between hydrogen atoms are small and the major part of the binding energy is from the energy of the CH bonds. The structures with three neighboring hydrogen atoms are not stable, because E_b for hydrogen atoms on the 1-2-3 sites is 2.22 eV. For the four neighboring hydrogen atom configurations, E_b for hydrogen atoms on the 1-2-3-7, 1-2-5-6, and 1-2-3-4 sites are 2.17, 2.15, and 2.48 eV, respectively. E_b for the 1-2-3-4 neighboring configuration is the largest, showing that the hydrogen dimers prefer to form chains along the axis of the tube, instead of cluster. There are three typical patterns for the hydrogen atoms on the walls of the carbon nanotubes: (a) the vertical chain pattern,[21] with every other carbon zigzag chain saturated by hydrogen atoms (2-3-6-7-10-11); (b) the dimer pattern,[21] with every other carbon dimer rows perpendicular to the zigzag carbon chains saturated by hydrogen atoms (1-2-5-6-9-10); (c) the parallel polyacetylene-like chains (1-2-3-4-9-10-11-12), which has been studied in the fluorinated SWCNT's.[22] We consider structures comprised of these three patterns. We have calculated the most probable structures with different coverages and atomic configurations in order to seek stable configurations. For a coverage of $x\leqslant 0.5$, hydrogen atoms prefer to form parallel polyacetylenelike chains. The chains are located symmetrically to minimize the total energies. For a coverage of $x=0.5$, pattern (c) is the most stable configuration with E_b of 2.44 eV. E_b of patterns (a) and (b) are 1.96 eV and 2.16 eV, respectively. For a coverage of $x>0.5$, we can use the complement any vacancy patterns to describe structures of the hydrogen adsorbates on the carbon nanotubes. It is found that the vacancies prefer to form pattern (b) and the vacancy dimers are located symmetrically. The structures on the other $(n,0)$ $(n=6,12,16)$ tubes are similar to those of the (8,0) tube. For the (n,n) tubes, hydrogen atoms prefer to form parallel polyacetylenelike chains (2-3-6-7). For a coverage of $x\leqslant 0.5$, the chains are located symmetrically to minimize the total energies. For a coverage of $x>0.5$, the vacancies prefer to form 1-2 dimers and the vacancy dimers are located symmetrically.

We have calculated the energies of different coverages according to the possible stable configurations. We define the intercalation energy as follows:[3]

$$E_I=(E_{SWCNT}+n_HE_H-E_{H\text{-}SWCNT})/n_C, \quad (1)$$

where n_C is the number of carbon atoms. Figure 2(a) shows the calculated E_I of the possible configurations of the (8,0) tubes. E_I depends on the coverage and the configurations. For a fixed coverage, we construct the possible structures with the three patterns and the structure with the highest E_I is the most stable one. For typical adsorbed systems, the number of ground states is finite and the stable coverage is discrete.[2] However, we find that there are a large number of ground states for the hydrogen adsorbates on SWCNT's and thus the intercalation energy varies smoothly as a function of stable coverage approximately. It is noted that the intercalation energy has an envelope profile which varies smoothly with hydrogen coverage, implying that stable hydrogen coverage can be considered as continuous approximately. We fit the profile of E_I with a polynomial function of power 3. The curves are plotted with solid lines in Fig. 2. As is shown in Fig. 2(a), the structures on the curve correspond to ground states and those under the curve correspond to unstable states. For exohydrogenated tubes, hydrogen atoms prefer to form chains along the axis of the tubes. The major part of the intercalation energy is from chains along the axis of the tubes. The curved surfaces of the tubes provide more degrees of freedom to reduce repulsions between the adsorbed

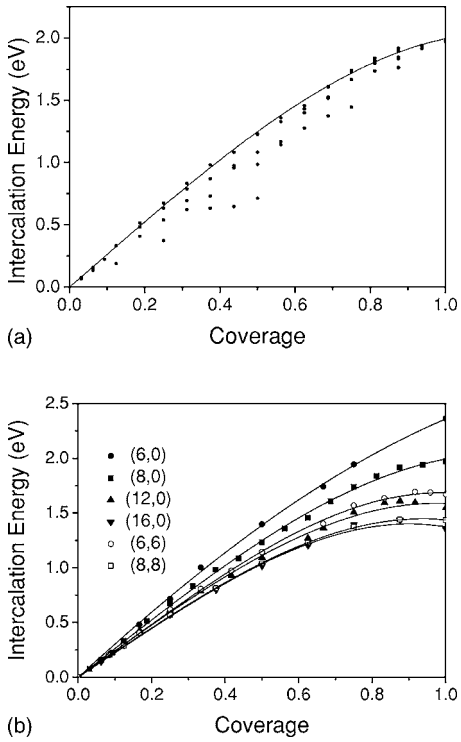

FIG. 2. (a) The intercalation energies of various structures of the hydrogenated (8,0) tube. (b) The intercalation energies of the stable structures of the hydrogenated carbon nanotubes with different diameters and chiralities.

atoms.[2] At low coverage, the interactions between the hydrogen dimers are weak and E_I increases linearly with the coverage. As the coverage increases, the distances between hydrogen atoms become shorter and the repulsions between hydrogen atoms become stronger. Thus, the profile of E_I turns flat. For the (12,0), (8,8), and (16,0) tubes, there is a peak value where E_I begins to descend, as is shown in Fig. 2(b). For the same coverage, the intercalation energy decreases with an increase of the nanotube diameter, which is in agreement with the results in Ref. 10.

In order to determine the dependence of the stability of the hydrogenated structures on temperature and pressure, we consider the hydrogen coverage dependence on the chemical potential. The Gibbs free energy difference ΔG for the formation of hydrogen adsorbates is given as follows:

$$\Delta G = E_{H\text{-}SWCNT} - E_{SWCNT} - x\mu_H, \tag{2}$$

where x is the hydrogen coverage and μ_H is the chemical potential of hydrogen atoms. μ_H depends on the temperature T and pressure P of the environment. The stable states are obtained by determining the minima of ΔG under the same chemical potential. We approximate the gas environment as an ideal gas; then, μ_H is given as

$$\mu_H = -k_B T \ln \frac{(2\pi m)^{3/2}(kT)^{5/2}}{Ph^3}, \tag{3}$$

where k_B is the Boltzmann constant, m is the mass of hydrogen atoms, and h is the Planck constant. In this model, $\mu_H < 0$ because $\mu_H = 0$ corresponds to a temperature of zero.

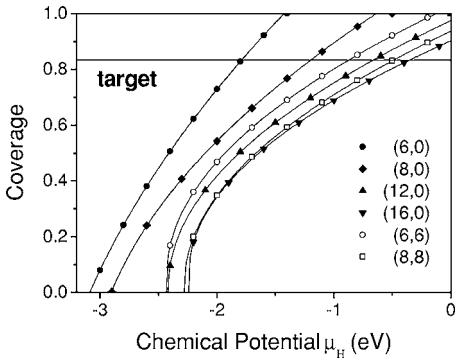

FIG. 3. The phase diagram of coverage vs chemical potential. Different symbols in the curves are used to distinguish the tubes.

Based on the envelope profile, we obtain a variation of the hydrogen coverage with a change of chemical potential as shown in Fig. 3. Hydrogen coverage of the stable states increases with an increase of the chemical potential μ_H. For the (6,0) tube, the hydrogen coverage x changes from 0 to 1 with an increase of the chemical potential μ_H from −3.10 eV to −1.42 eV. When the chemical potential $\mu_H \geqslant -1.78$ eV, the coverage reaches 83.4 at. %, which is higher than the target for practical applications.[6] For the (8,0) and (6,6) tubes, the corresponding chemical potential conditions are $\mu_H \geqslant -1.20$ eV and $\mu_H \geqslant -0.67$ eV, respectively. The interval of the chemical potential for applications is reduced with an increase of the nanotube diameter. As the temperature approaches zero, $\mu_H \to 0$ and hydrogen coverage on the SWCNT's reaches a maximum. For the (6,0), (8,0), and (6,6) tubes, the saturation hydrogen coverages are $x=1$. For the (12,0), (16,0), and (8,8) tubes, the saturation hydrogen coverages are $x=0.966$, $x=0.887$, and $x=0.937$, respectively. The saturation hydrogen coverage decreases with an increase of the nanotube diameter. The SWCNT's with smaller diameter are more efficient for hydrogen storage.

In the following, we analyze the variation of the hydrogen coverage with a change of temperature and pressure. Under ambient temperature and pressure of 1×10^{-9} Torr, 65 ± 15 at. % hydrogenation of carbon atoms has been obtained in SWCNT's with the diameters from 1 to 1.8 nm experimentally.[16] Figure 4 shows the coverage as a function of temperature at the experimental pressure. The hydrogen

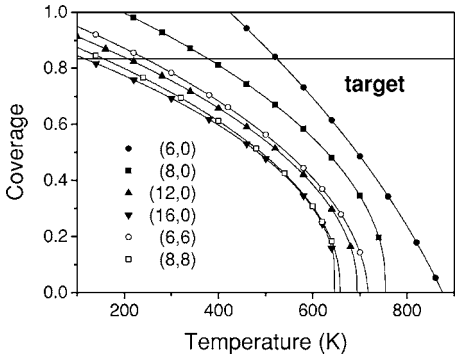

FIG. 4. The phase diagram of coverage vs temperature at the pressure of 1×10^{-9} Torr. Different symbols in the curves are used to distinguish the tubes.

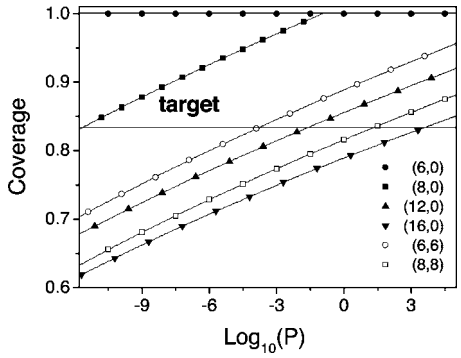

FIG. 5. The phase diagram of coverage vs the logarithm of pressure at the temperature of 300 K. The unit of pressure is pascal. Different symbols in the curves are used to distinguish the tubes.

coverage decreases as the temperature increases. For the (12,0) tube with a diameter of 9.4 Å, the hydrogen coverage is $x=0.78$ in the experiment conditions, which is in agreement with the experiment.[16] To achieve the target for practical applications, the temperature should be lower than 500 K for the (6,0) tube and 400 K for the (8,0) tube. With an increase of the nanotube diameter, the corresponding temperature decreases. At ambient temperature ($T=300$ K), we obtain the phase diagram of coverage versus pressure. As is shown in Fig. 5, the hydrogen coverage increases as the pressure increases. For $p \geqslant 10^{-12}$ Pa, the hydrogen coverages on the (6,0) and (8,0) tubes are higher than 83.4 at. %, showing the possibility in practical applications. For the (6,6) tube, the pressure should be higher than 10^{-5} Pa. With an increase of the nanotube diameter, the corresponding pressure becomes higher. For the hydrogen coverage on the (16,0) tube to reach the target for applications, the pressure should be higher than 10^3 Pa.

IV. SUMMARY

In summary, we have performed calculations on atomic hydrogen adsorption on the walls of carbon nanotubes with various diameters and chiralities. We find hydrogen atoms prefer to form chains on the walls of the tubes. We show that the wall curvature of the tubes reduces the repulsions between the adsorbed atoms and thus the intercalation energy decreases with an increase of the nanotube diameter. The full hydrogen coverage can be reached for nanotubes with small size, while for nanotubes with large size, the saturation coverage is lower than 1. We obtain the phase diagrams of the hydrogen coverage as a function of the chemical potential. We have determined the variation of the hydrogen coverage with the change of temperature and pressure. We find that carbon nanotubes with diameters of about 1 nm can achieve a coverage of 80% at ambient temperature and low pressure, which is in agreement with a recent experiment.[16] The capacity of hydrogen storage depends strongly on the diameters of the tubes. Hydrogen capacity in small carbon nanotubes exceeds 6.5 wt % at ambient temperature, which implies great potential for practical applications.

ACKNOWLEDGMENTS

This research was supported by the National Natural Science Foundation of China under Grant No. 10474049, and National Basic Research Program of China (No. 2006CB605105) and the Key Grant Project of Chinese Ministry of Education (No. 306020).

[1] S. Louis and Z. Andreas, Nature (London) **414**, 353 (2001).
[2] X. Yang and J. Ni, Phys. Rev. B **69**, 125419 (2004).
[3] J. Zhao, A. Buldum, J. Han, and J. P. Lu, Phys. Rev. Lett. **85**, 1706 (2000).
[4] S. M. Lee and Y. H. Lee, Appl. Phys. Lett. **76**, 2877 (2000).
[5] P. Chen *et al.*, Science **285**, 91 (1999).
[6] W. Q. Deng, X. Xu, and William A. Goddard III, Phys. Rev. Lett. **92**, 166103 (2004).
[7] Y. Zhao, Y. H. Kim, A. C. Dillon, M. J. Heben, and S. B. Zhang, Phys. Rev. Lett. **94**, 155504 (2005).
[8] T. Yildirim and S. Ciraci, Phys. Rev. Lett. **94**, 175501 (2005); T. Yildirim, J. Iniguez, and S. Ciraci, Phys. Rev. B **72**, 153403 (2005).
[9] G. Chen, X. G. Gong, and C. T. Chan, Phys. Rev. B **72**, 045444 (2005).
[10] Y. Ye, C. C. Ahn, C. Witham, B. Fultz, J. Liu, A. G. Rinzler, D. Colbert, K. A. Smith, and R. E. Smalley, Appl. Phys. Lett. **74**, 2307 (1999).
[11] J. Lawrence and G. Xu, Appl. Phys. Lett. **84**, 918 (2004).
[12] T. Yildirim, O. Gulseren, and S. Ciraci, Phys. Rev. B **64**, 075404 (2001).
[13] S. M. Lee, K. H. An, Y. H. Lee, G. Seifert, and T. Frauenheim, J. Am. Chem. Soc. **123**, 5059 (2001).
[14] K. A. Park, K. Seo, and Y. H. Lee, J. Phys. Chem. B **109**, 8967 (2005).
[15] C. W. Bauschlicher and C. R. So, Nano Lett. **2**, 337 (2002).
[16] A. Nikitin, H. Ogasawara, D. Mann, R. Denecke, Z. Zhang, H. Dai, K. Cho, and A. Nilsson, Phys. Rev. Lett. **95**, 225507 (2005).
[17] G. Kresse and J. Hafner, Phys. Rev. B **47**, R558 (1993); **49**, 14251 (1994); G. Kresse and J. Furthmüller, Comput. Mater. Sci. **6**, 15 (1996); Phys. Rev. B **54**, 11169 (1996).
[18] D. Vanderbilt, Phys. Rev. B **41**, R7892 (1990).
[19] J. P. Perdew, J. A. Chevary, S. H. Vosko, K. A. Jackson, M. R. Pederson, D. J. Singh, and C. Fiolhais, Phys. Rev. B **46**, 6671 (1992).
[20] H. J. Monkhorst and J. D. Pack, Phys. Rev. B **13**, 5188 (1976).
[21] O. Gulseren, T. Yildirim, and S. Ciraci, Phys. Rev. B **66**, 121401(R) (2002).
[22] G. Seifert, T. Kohler, and T. Frauenheim, Appl. Phys. Lett. **77**, 1313 (2000).